https://doi.org/10.5194/egusphere-2026-5144
Preprint. Discussion started: 8 September 2026

Sensitivity of the Lagrangian temperature anomaly decomposition to model choice: Lessons from the 2021 Pacific Northwest heatwave

Albenis Pérez-Alarcón[1], Raquel Nieto[1,2], Luis Gimeno[1,2]

[1]Centro de Investigación Mariña, Universidade de Vigo, Environmental Physics Laboratory (EPhysLab), Campus As Lagoas s/n, 32004 Ourense, Spain.
[2]Climate System Research Unit, UVigo-CESGA, Santiago de Compostela, Spain

Correspondence to: Albenis Pérez-Alarcón (albenis.perez.alarcon@uvigo.es)

Abstract. The Lagrangian temperature anomaly decomposition has emerged as a powerful tool for quantifying the relative importance of adiabatic, advective and diabatic processes during heatwaves. However, its sensitivity to the choice of Lagrangian model, whether pure-trajectory or dispersion-based, remains poorly understood. Using seven different trajectory sets, we apply this decomposition to the June 2021 Pacific Northwest heatwave to examine discrepancies in process attribution across model classes. Pure-trajectory models consistently identify diabatic heating as the dominant contributor, whereas dispersion models attribute the largest fraction to adiabatic warming. A trajectory cluster analysis and parcel position diagnostics reveal that this divergence does not stem from different geographic origins or the near-surface vertical distribution over the target region during the heatwave, which are broadly similar across trajectory sets, but from contrasting vertical histories. While dispersion-model parcels reside at higher altitudes before arrival, exposing them to subsidence warming, pure-trajectory parcels remain near the surface where land–atmosphere feedbacks and antecedent dry soils amplify diabatic heating. These findings demonstrate that this Lagrangian framework is fundamentally sensitive to model choice, particularly to the representation of turbulent motion, which induce parcel vertical dispersion absent in the resolved wind fields. While this study does not establish which Lagrangian model class is most suitable, it represents a first step toward understanding these discrepancies and cautions that heatwave attribution studies relying on a single Lagrangian model should interpret inferred process dominance carefully, as it may reflect methodological choices rather than the underlying physics alone.

1 Introduction

Heatwaves (HWs) are one of the most dangerous natural hazards worldwide (Perkins, 2015; Pascaline and Rowena, 2018; Barriopedro et al., 2023), typically defined as prolonged periods of abnormally high temperatures that exceed certain thresholds relative to the local climatology (Robinson, 2001; Di Luca et al., 2020; Barriopedro et al., 2023). The impacts of HWs are severe and multifaceted, ranging from direct heat-related illnesses and deaths (Ebi et al., 2021; Neal et al., 2022) to indirect consequences such as agricultural losses (Brás et al., 2021; Breshears et al., 2021; De Lima et al., 2021; Font et al., 2021), wildfires (Moritz et al., 2005; Ruffault et al., 2017, 2020; Sutanto et al., 2020; Mario et al., 2024), and infrastructure failures

https://doi.org/10.5194/egusphere-2026-5144
Preprint. Discussion started: 8 September 2026

(Vogel et al., 2019; Stone et al., 2021). Among the most devastating heat waves in recent history are the European HW of 2003, which caused approximately 40 000 excess deaths (Alcamo et al., 2007; García-Herrera et al., 2010), the Russian HW of 2010 that resulted in over 55 000 fatalities, widespread wildfires, and major crop failure (Barriopedro et al., 2011), and the June 2021 Pacific Northwest (PNW21) HW, which shattered temperature records by unprecedented margins and caused catastrophic damage in the town of Lytton, British Columbia (Neal et al., 2022; Philip et al., 2022; White et al., 2023; Fleishman et al., 2025).

Recent advances in understanding HWs have increasingly employed Lagrangian methods, which track individual air parcels backwards in time to identify their origins and the physical processes that modify their thermodynamic properties en route to the HW region (Gimeno et al., 2026). Bieli et al. (2015) pioneered the use of Lagrangian backward trajectories to characterise air masses associated with Central European temperature extremes, demonstrating that hot extremes occur near the centres of blocking anticyclones, where high temperatures result from adiabatic warming in descending air masses, as well as from diabatic heating by radiation and surface fluxes. Santos et al. (2015) applied this framework to study the mechanisms leading to temperature extremes in the Iberian Peninsula. Quinting and Reeder (2017) employed a similar trajectory-based approach to southeastern Australian HWs, highlighting the role of adiabatic compression during these events. Zschenderlein et al. (2020) further established that European heat waves are consistently associated with upper-tropospheric anticyclones whose formation depends on latent heating within extratropical cyclones and whose maintenance relies on convection-driven diabatic heating, traced through seven-day backward trajectories initialised in the anticyclones. Schumacher et al. (2019, 2020) subsequently developed a Lagrangian framework analogous to the moisture source identification to estimate the origins of sensible heat that contribute to temperature extremes, thereby enabling quantification of heat source-receptor relationships from air parcel trajectories. A combined Lagrangian analysis of moisture and heat sources was recently employed by Li et al. (2024) to examine yield deficits across Australia's largest rainfed wheat-producing region, whereas Zhou et al. (2024) applied the heat-tracking methodology developed by Schumacher et al. (2019) to explore the relationship between upwind drought conditions and heat wave events in East China. Meanwhile, Pérez-Alarcón et al. (2025a) tracked atmospheric moisture and heat to examine compound drought-heat wave events in the Iberian Peninsula.

While it is widely accepted that HWs are mainly triggered by horizontal transport of warm air (Sousa et al., 2019; Tamarin-Brodsky et al., 2020), atmospheric subsidence (Zhou and Yuan, 2022; Röthlisberger and Papritz, 2023), and diabatic heating (Zhou et al., 2019; Miralles et al., 2019; Wehrli et al., 2022), a key limitation of the aforementioned Lagrangian trajectory-based studies is that they do not allow for the quantification of the contributions of these processes to the temperature anomaly. In this context, Röthlisberger and Papritz (2023) introduced a novel temperature anomaly decomposition approach that quantifies their relative contributions. This framework has been increasingly applied in recent studies to examine HWs across different regions. For instance, Fernandez-Alvarez (2025, 2026) identified adiabatic warming as the dominant heat driver during the record-breaking 2023 Amazon drought and the 2022 European mega-drought. Similarly, Pérez-Alarcón et al. (2025b) examined the importance of these processes during the May 2024 HW in Cuba, finding that adiabatic processes were the principal air-warming mechanism. Conversely, Oppong et al. (2025) found that extreme HWs in the Caribbean region are

https://doi.org/10.5194/egusphere-2026-5144
Preprint. Discussion started: 8 September 2026

mainly driven by diabatic processes, with a lower contribution from adiabatic warming. Similar results were reported by Lemburg et al. (2026) for near-surface temperature anomalies during central European omega-type HWs and by Röthlisberger and Papritz (2023) for the PNW21 HW. In addition, Hotz et al. (2024) applied the decomposition to examine the vertical structure of temperature anomalies during recent HW events, providing nuanced insights into how vertical motion modulates temperature anomalies within anticyclones. A key theoretical development was introduced by Mayer and Wirth (2025), who proposed two different perspectives for understanding HWs within the Lagrangian framework, using an Eulerian method based on tracer advection. Their study demonstrated that characterising these temperature extremes from a Lagrangian viewpoint is highly sensitive to the approach adopted, with two distinct methods yielding substantial differences regarding the relative importance of the contributing processes. These findings carry profound implications for the interpretation of Lagrangian HW studies, underscoring the need for careful consideration of the methodological framework employed.

An additional layer of complexity arises from the observation that studies applying the temperature anomaly decomposition approach using different Lagrangian models have reached divergent conclusions regarding the dominant physical processes contributing to HWs. Specifically, those using air parcel trajectories from the Lagrangian FLEXible PARTicle dispersion (FLEXPART) model (Pisso et al., 2019; Bakels et al., 2024) have often shown that adiabatic processes are the main contributor to temperature anomalies during HWs (e.g., Fernández-Alvarez et al., 2025, 2026; Pérez-Alarcón et al., 2025b). In contrast, studies using the Lagrangian analysis tool (LAGRANTO; Sprenger and Wernli, 2015) have frequently identified diabatic processes as the main contributor to temperature anomalies (Röthlisberger and Papritz, 2023; Lemburg et al., 2026). The divergence in findings between models can be partly understood through the physical mechanisms typically associated with HWs, the specific characteristics of the Lagrangian model employed, and how air parcel trajectories are computed. These events mostly occur under the influence of persistent high-pressure systems, which are characterised by sinking air, clear-sky conditions, and suppressed cloud formation (Pfahl and Wernli, 2012; Schaller et al., 2018; Sousa et al., 2018; Barriopedro et al., 2023). These conditions favour adiabatic warming as air parcels descend and compress under the anticyclonic circulation. Simultaneously, the clear skies and strong insolation associated with high-pressure systems enhance surface sensible heat fluxes, which through land–atmosphere feedbacks can significantly contribute to near-surface warming, particularly when antecedent soil moisture deficits reduce evaporative cooling and amplify sensible heat release (Fischer et al., 2007; Berg et al., 2014; Stéfanon et al., 2014; Miralles et al., 2014, 2019).

Global warming is altering weather and climate variability while intensifying extreme events such as HWs, with progressively stronger impacts on the Earth system projected for the future (Dosio et al., 2018; He et al., 2023; Jia et al., 2026). Consequently, differences in reported contributions from studies using different Lagrangian models warrant further examination to clarify how adiabatic, advective, and diabatic processes contribute to HW development. This study compares the temperature anomaly decomposition results using LAGRANTO, FLEXPART, the Hybrid Single-Particle Lagrangian Integrated Trajectory (HYSPLIT) model (Stein et al., 2015), and the Hybrid Parcel Tracker (HPT; Shukla et al., 2026) for the PNW21 HW event. The main goal of this study is to provide an initial assessment of how model-specific characteristics influence the quantification

https://doi.org/10.5194/egusphere-2026-5144
Preprint. Discussion started: 8 September 2026

of adiabatic, advective, and diabatic contributions to temperature anomalies and to lay groundwork for interpreting Lagrangian HW analyses across different modelling frameworks.

2 Methods

2.1 Study case

We selected the PNW21 HW peak (28–30 June 2021) as our case study, as it is one of the most extreme on record and among the most extensively documented in the literature (e.g., McKinnon and Simpson, 2022; Neal et al., 2022; Schumacher et al., 2022; Baier et al., 2023; Oertel et al., 2023; White et al., 2023; Mass et al., 2024; Fleishman et al., 2025). Near-surface temperature anomalies reached 16–20°C above normal across a broad region, with numerous locations shattering all-time maximum temperature records by more than 5°C (White et al., 2023; Bair et al., 2023). The Canadian national temperature record was broken on three consecutive days, peaking at 49.6°C in Lytton, British Columbia, on 29 June (White et al., 2023). The event was mainly driven by an exceptionally strong ridge of high pressure in the middle and upper troposphere, consistent with a persistent Omega block over the northeastern Pacific and western North America (Schumacher et al., 2022; Mass et al., 2024). The ridge strengthened rapidly beginning on 24 June, peaked over southern British Columbia on 27 June with record-breaking 500-hPa geopotential heights, and induced widespread tropospheric subsidence (Mass et al., 2024). In addition, an anomalously strong East Asian jet stream and a northward-propagating monsoon rain belt forced a trans-Pacific Rossby wave train across the North Pacific (Qian et al., 2022). Concurrently, an unusually strong atmospheric river making landfall in Alaska transported low-latitude air poleward toward the northeast Pacific, while increased water vapour within the ridge enhanced the short-term greenhouse effect (Baier et al., 2023; Lin et al., 2022). At the surface, a strong thermal trough parallel to the Oregon coast blocked cooler marine air from penetrating inland (Fleishman et al., 2025). Moreover, clear-sky conditions contributed to anomalously high downward shortwave radiation (Terray, 2023). These conditions, together with anomalous soil moisture deficit (Conrick and Mass, 2023) and related land-atmosphere feedback (e.g., Stéfanon et al., 2014; Miralles et al., 2014) contributed to the event's magnitude and persistence. Further details of the PNW21 HW can be found in Fleishman et al. (2025).

2.1 Lagrangian Models

In this study, we use air parcel trajectories from different simulations and Lagrangian models to quantify the relative contributions of advective, adiabatic, and diabatic processes during the 2021 PNW HW (28–30 June) by applying the Lagrangian temperature anomaly decomposition approach (Röthlisberger and Papritz, 2023). Using multiple set of air parcel trajectories allows us to assess the sensitivity of the decomposition to model-specific characteristics, including trajectory calculation schemes and parameterisations of subgrid-scale processes.

https://doi.org/10.5194/egusphere-2026-5144
Preprint. Discussion started: 8 September 2026

2.2.1 LAGRANTO

LAGRANTO is a Lagrangian trajectory model (Sprenger and Wernli, 2015) that calculates three-dimensional kinematic backwards and forward trajectories by integrating the horizontal wind components and vertical velocity from meteorological reanalysis or model output. LAGRANTO does not parameterise subgrid-scale convection; instead, trajectories are driven solely by the resolved large-scale wind fields. In this work, we used the LAGRANTO simulations provided by Röthlisberger and Papritz (2023), which were driven by 3-hourly data from the ERA5 reanalysis of the European Centre for Medium-Range Weather Forecasts (ECMWF; Hersbach et al., 2020) on model levels at a 0.5° × 0.5° horizontal grid. The 15-day backward trajectories were started at each ERA5 grid point at 6-hourly intervals near the surface at 10, 30, and 50 hPa above ground level within the domain bounded by 100°–140°W and 35°–70°N.

2.2.2 FLEXPART

FLEXPART is a Lagrangian particle dispersion model (Stohl et al., 1998; Pisso et al., 2019; Bakels et al., 2024) originally developed for investigating the dispersion of atmospheric pollutants, which has evolved into an essential tool for simulating and analysing atmospheric transport processes, including moisture and heat tracking. FLEXPART calculates particle trajectories using a zero-acceleration scheme (Stohl et al., 2005), where the wind vector consists of a grid-scale component, a turbulence component, and an optional mesoscale wind disturbance component (optional from version 11 onward; in earlier versions, mesoscale turbulence is always active). The model includes parameterisations of turbulence in the atmospheric boundary layer based on Hanna (1982) and Ryall and Maryon (1998) schemes, with added features from Cassiani et al. (2015) for skewed turbulence conditions. Above the boundary layer, turbulent velocities are computed following (Legras et al. 2003). Mesoscale turbulence is parameterised using the method described by Maryon (1998), which involves the standard deviation of wind velocities at surrounding grid points. Meanwhile, vertical transport by moist subgrid-scale convection is parameterized using the scheme proposed by Emanuel and Živković-Rothman (1999).

In this study, we used four different sets of forward FLEXPART simulations with domain-filling global runs. In all cases, the model was driven by 3-hourly ERA5 reanalysis data on a 0.5° × 0.5° horizontal grid. The first dataset was produced with FLEXPART-v10.4, releasing 30 million air parcels (Vázquez et al., 2024); the second was produced with FLEXPART-v11, with 20 million air parcels (Deman et al., 2026). The third dataset was the LARA reanalysis (Bakels et al., 2025), derived using FLEXPART-v11 with 6 million air parcels. The v10.4 and v11 datasets were generated year by year to prevent the progressive degradation of particle distribution that occurs during extended continuous runs (Bakels et al., 2024). Finally, the fourth dataset was obtained by running FLEXPART-v11 from 1 June to 3 July 2021 with all subgrid-scale parameterisations switched off, including turbulence, mesoscale turbulence, convection, and subgrid orographic boundary-layer height, forcing purely kinematic trajectories driven exclusively by the resolved large-scale wind fields (hereafter FLEXPART-TRJ). For the four datasets, air parcels trajectories reaching the target region (100°–140°W and 35°–70°N) near-surface (up to 50 hPa above the

https://doi.org/10.5194/egusphere-2026-5144
Preprint. Discussion started: 8 September 2026

surface; Mayer and Wirth, 2025) during the HW dates were extracted using the Lagrangian atmospheric moisture and heat tracking tool (LATTIN; Pérez-Alarcón et al., 2024, 2026).

2.2.3 HYSPLIT

HYSPLIT is a widely used trajectory and dispersion model that computes air parcel trajectories by integrating the three-dimensional wind field. HYSPLIT can be run in either trajectory mode, which calculates the path of air parcels, or dispersion mode, which simulates transport and dispersion processes (Stein et al., 2015). In trajectory mode, HYSPLIT computes backwards or forward trajectories using meteorological data interpolated to the parcel position. Unlike FLEXPART, HYSPLIT in trajectory mode does not include explicit parameterisations of subgrid-scale turbulence or convection; instead, it relies on the resolved wind fields from the meteorological input data. In this study, we used HYSPLIT in trajectory mode driven by 3-hourly Global Forecast System (GFS) data on a 0.25° horizontal grid spacing. The 15-day backward trajectories were started at every 0.25° grid point at 6-hourly intervals near the surface at 10, 30, and 50 hPa above ground level.

2.2.4 HPT

HPT is a recently developed Lagrangian framework (Shukla et al., 2026) that traces forward air parcel trajectories by integrating the three-dimensional wind field. By excluding parameterisations for subgrid-scale turbulence, aerosol transport, and chemical dispersion, HPT provides a simplified yet physically focused and computationally efficient approach for hydro-meteorological and temperature-extreme research. In this study, we conducted a global HPT simulation using 3-hourly ERA5 data at a horizontal grid spacing of 0.25°. The simulation period was from June 10 to July 1, 2021. Air parcels were released at each grid point at 22 pressure levels ranging from 200 to 1000 hPa (in 50 hPa increments, with additional levels at 775, 825, 875, 925 and 975 hPa). Following the same procedure as for FLEXPART, we filtered air parcels that reached the target region during the heat wave using the LATTIN tool.

2.3 Lagrangian temperature anomaly decomposition

The temperature anomaly (T') decomposition approach follows the methodology of Röthlisberger and Papritz (2023), which integrates the material change of the Lagrangian temperature anomaly along kinematic backward trajectories.

$$T'(x,t) - T'(x_g,t_g) = -\int_{t_g^{sea}}^{t} \frac{\partial \overline{T}}{\partial t} d\tau - \int_{t_g^{adv}}^{t} v \cdot \nabla_h(\overline{T}) d\tau + \int_{t_g^{adi}}^{t} \left[\frac{\kappa T}{p} - \frac{\partial \overline{T}}{\partial p} \right] \omega d\tau + \int_{t_g^{dia}}^{t} \left(\frac{p}{p_0} \right)^{\kappa} \frac{D\theta}{Dt} d\tau \quad (1)$$

https://doi.org/10.5194/egusphere-2026-5144
Preprint. Discussion started: 8 September 2026

The resulting equation yields four terms in the right hand side (from right to left): a seasonality term (seasonality T') that accounts for temporal changes of the climatology and the contribution from the diurnal cycle of $\overline{T}$; an advective term (advective T') quantifying how T' is affected by horizontal advection across climatological temperature gradients; an adiabatic term (adiabatic T') combining the effects of vertical advection of climatological $\overline{T}$ and adiabatic compression or expansion; and a diabatic term (diabatic T') representing changes in potential temperature due to diabatic heating from radiation, surface sensible heat fluxes, and turbulent mixing. The climatological temperature $\overline{T}$ is computed by averaging each three-hourly time step over a running 31-day window and a 30-year period (1991-2020). Meanwhile, $\frac{\partial \overline{T}}{\partial t}$ and $\frac{\partial \overline{T}}{\partial p}$ are computed on the basis of first-order (centred) finite differences. By integrating Eq. 1 from the genesis time t_g to t, we can quantify the relative contributions of advective, adiabatic, and diabatic processes to temperature anomalies. Further details on this approach can be found in Röthlisberger and Papritz (2023). This framework has been implemented in the LATTIN tool.

3 Results and discussion

3.1 Lagrangian temperature anomaly decomposition

Figure 1 shows the six-hourly averaged Lagrangian temperature anomaly decomposition for the PNW HW event from 28 June 00 UTC to 30 June 18 UTC. The decomposition is evaluated across seven distinct trajectory sets, grouped into four pure trajectory models (LAGRANTO, HYSPLIT, HPT and FLEXPART-TRJ) and three Lagrangian particle dispersion simulations (FLEXPART-10.4, FLEXPART-11 and LARA). All configurations capture the gross spatial structure of the total temperature anomaly, with a pronounced warm core exceeding 12 K (solid contour in Figure 1), peaking near Lytton, British Columbia (Röthlisberger and Papritz, 2023). Although the LARA-based decomposition exhibits somewhat larger deviations in the fine-scale structure, this can be attributed to the comparatively modest number of particles tracked in the LARA reanalysis, which limits the effective spatial resolution for individual case studies (Bakels et al., 2025). Figure 1 reveals a striking and systematic divergence in the attribution of the heatwave to individual physical processes: the pure trajectory models consistently identify diabatic processes as the dominant contributor to the temperature anomalies, whereas the dispersion models attribute the largest fraction of the warming to adiabatic heating. Meanwhile, the advective contribution shows a dipole structure of cold-air advection flanking the warm core in all configurations, while the seasonality term is uniformly weak.

Despite the differences in the leading-order physical process, the reconstructed budget sums remain in close agreement across all models and closely match the observed total temperature anomaly, indicating that secondary contributions largely compensate for discrepancies between individual process terms. This close agreement further indicates that the decomposition is physically consistent. Minor differences arise from the residual term inherent in the Lagrangian temperature anomaly decomposition, which in most instances remains below 0.5 K but can exceed this threshold when a parcel's temperature anomaly stays positive throughout the entire 15-day backward integration (Papritz and Röthlisberger, 2023; Röthlisberger and

https://doi.org/10.5194/egusphere-2026-5144
Preprint. Discussion started: 8 September 2026

Papritz, 2023; Lemburg et al., 2026). Overall, the differences in the relative contributions of adiabatic, advective and diabatic processes shown in Figure 1 suggest that the Lagrangian temperature anomaly decomposition is sensitive to how sub-grid turbulence and convection are represented or neglected in the model simulations.

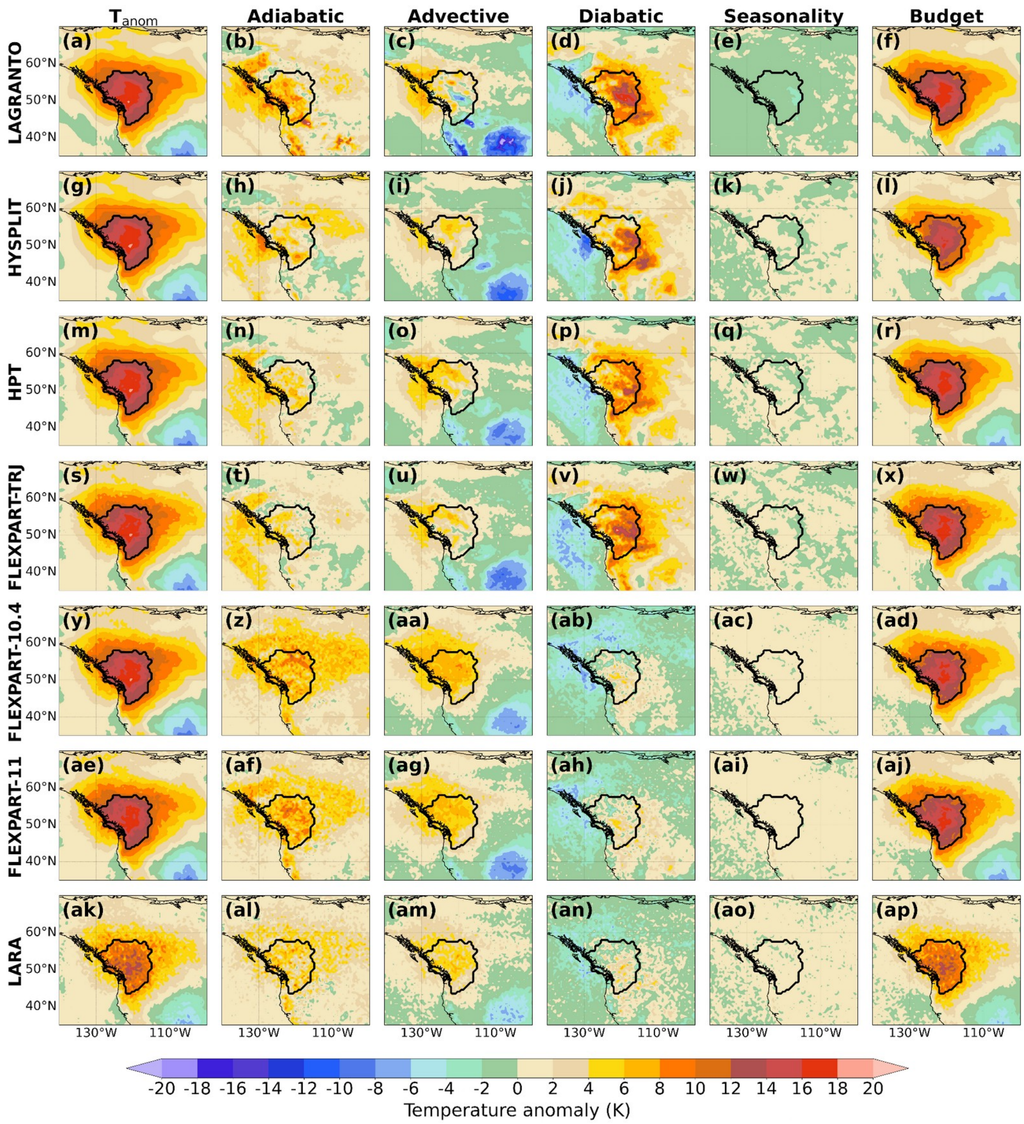

Figure 1: Lagrangian temperature anomaly decomposition during the 28–30 June 2021 Pacific Northwest heatwave. Each row corresponds to a different Lagrangian trajectory model or configuration (from top to bottom: LAGRANTO, HYSPLIT, HPT, FLEXPART-TRJ, FLEXPART-10.4, FLEXPART-11, and LARA). Columns show (left to right): the total temperature anomaly, and its Lagrangian decomposition into Adiabatic, Advective, Diabatic, and Seasonality contributions, together with the reconstructed budget (sum of the four

https://doi.org/10.5194/egusphere-2026-5144
Preprint. Discussion started: 8 September 2026

right-hand terms). All fields are averaged over 6-hourly outputs from 28 June 00 UTC to 30 June 18 UTC. The solid black contour encloses regions where the total temperature anomaly exceeds 12 K based on the LAGRANTO anomaly decomposition.

To gain further insight into the relative importance of each physical process across pure trajectory and dispersion models, Figure 2 shows the relative contribution of adiabatic, diabatic, advective and seasonality terms to the temperature anomaly, computed at each grid point within the 12 K contour area identified in Figure 1 and subsequently averaged across all 6-hourly time steps from 28 June 00 UTC to 30 June 18 UTC. The violin distributions reveal a marked and systematic dichotomy between model classes that corroborates the spatial patterns shown in Figure 1. Among the pure trajectory models, diabatic processes constitute the dominant contribution, with mean fractions ranging from 38% in HYSPLIT to 57% in LAGRANTO and FLEXPART-TRJ, whereas adiabatic heating remains comparatively modest (10–26%). These findings align with previous analyses of the PNW21 event. For instance, Röthlisberger and Papritz (2023) reported contributions of 59.2% diabatic, 37.7% adiabatic and 9.5% advective, consistent with the diabatic-dominant behaviour of the pure trajectory models. Schumacher et al. (2022) employed TRACMASS (Aldama-Campino et al., 2020; Döös, 1995) to trace air masses backward for 15 days and identified intense upwind latent heating over the North Pacific, fueled by tropical air masses ascending in warm conveyor belts, as a key driver of the anomalously warm troposphere, followed by adiabatic warming through subsidence within the anticyclone and downward mixing via deep boundary layers. Their trajectory-based perspective thus highlights the importance of both diabatic and adiabatic processes throughout the air-mass history, complementing the diabatic-dominant view of pure trajectory models while underscoring the role of remote advective transport. White et al. (2023) used HYSPLIT trajectories to estimate that approximately 78% of the net temperature change was attributed to diabatic processes and 22% to adiabatic subsidence; however, their study applied a different Lagrangian decomposition approach focused exclusively on adiabatic and diabatic processes, without separating advective and seasonality terms. This methodological distinction likely accounts for the higher diabatic fraction in their analysis relative to our HYSPLIT result. The resulting budget from pure-trajectory models converges with the Eulerian tracer-advection analysis by Mayer and Wirth (2025), who found that diabatic heating was the largest process contributing to near-surface potential temperature anomalies during the HW, further supporting the diabatic-dominant perspective from an independent, non-trajectory-based framework.

https://doi.org/10.5194/egusphere-2026-5144
Preprint. Discussion started: 8 September 2026

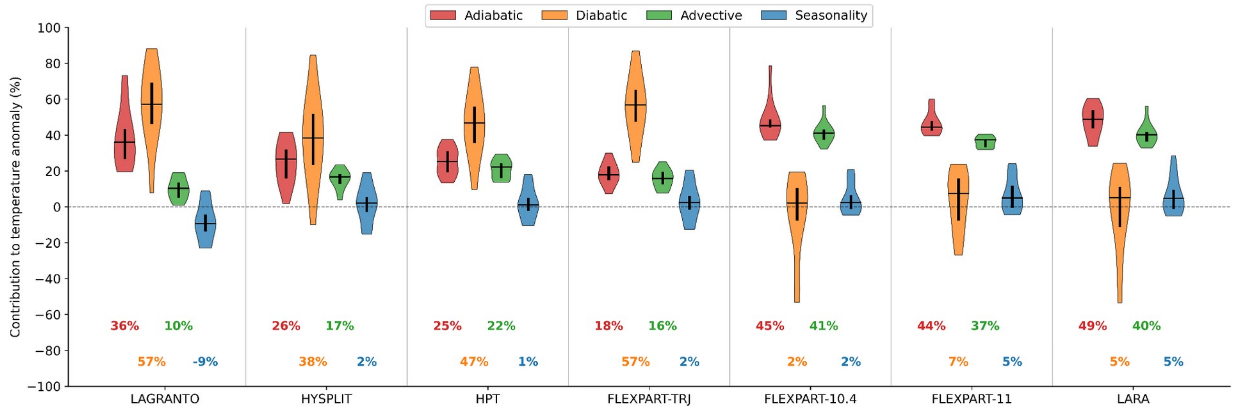

Figure 2: Relative contribution (%) of individual processes to the temperature anomaly within the 12 K contour area during the 28–30 June 2021 Pacific Northwest heatwave. Contributions were computed at each grid point within the 12 K contour (Figure 1) and spatially averaged for each 6-hourly time step from 28 June 00 UTC to 30 June 18 UTC. Violin plots show the distribution across the 12 six-hourly averages, with black horizontal bars indicating the median and black vertical bars the interquartile range. Coloured numbers at the bottom denote the median contribution (%) of each process across all time steps.

By contrast, when the Lagrangian temperature anomaly decomposition framework is applied to the dispersion models (FLEXPART-10.4, FLEXPART-11 and LARA), the results attribute the largest share of the warming to adiabatic processes (44–49%), accompanied by substantial advective contributions (37–41%) and only minor diabatic heating (2–7%). Notably, Baier et al. (2023) employed FLEXPART as a Lagrangian particle dispersion model to examine the deep tropical origin of the air masses during this event. They identified anomalous advection of sensible and latent heat from the tropics as the dominant process, with latent heat efficiently converted to sensible heat through precipitation. This emphasis on advective transport is qualitatively consistent with the substantial advective fractions in our dispersion-model results, though direct quantitative comparison is precluded by their receptor-oriented framework. Overall, these findings underscore that the inferred process contributions are sensitive to both the trajectory model class and the specific decomposition framework employed, in agreement with Mayer and Wirth (2025).

3.2 Parcel distributions and trajectory characteristics

To investigate the origin of the systematic differences in process attribution between pure trajectory and dispersion models, Figure 3 shows the three-dimensional distribution of Lagrangian parcels within the 12 K temperature anomaly contour (Figure 1) at 00 UTC on 29 June 2021. Across all seven configurations, the parcels exhibit a broadly similar bimodal vertical structure, and median pressures ranging from 866 hPa (LAGRANTO) to 881 hPa (HPT). This behaviour is further corroborated when analyzing the vertical distribution of all parcels within the 12 K contour from 28 to 30 June 2021, as shown in Figure 3h. Notably, dispersion models and pure trajectory models sample highly similar vertical and horizontal positions within the target region. This similarity in parcel distributions indicates that the divergence in diagnosed adiabatic, diabatic, and advective

https://doi.org/10.5194/egusphere-2026-5144
Preprint. Discussion started: 8 September 2026

contributions is not primarily a consequence of different spatial or vertical sampling of the air masses over the region of interest when initializing the backward trajectories.

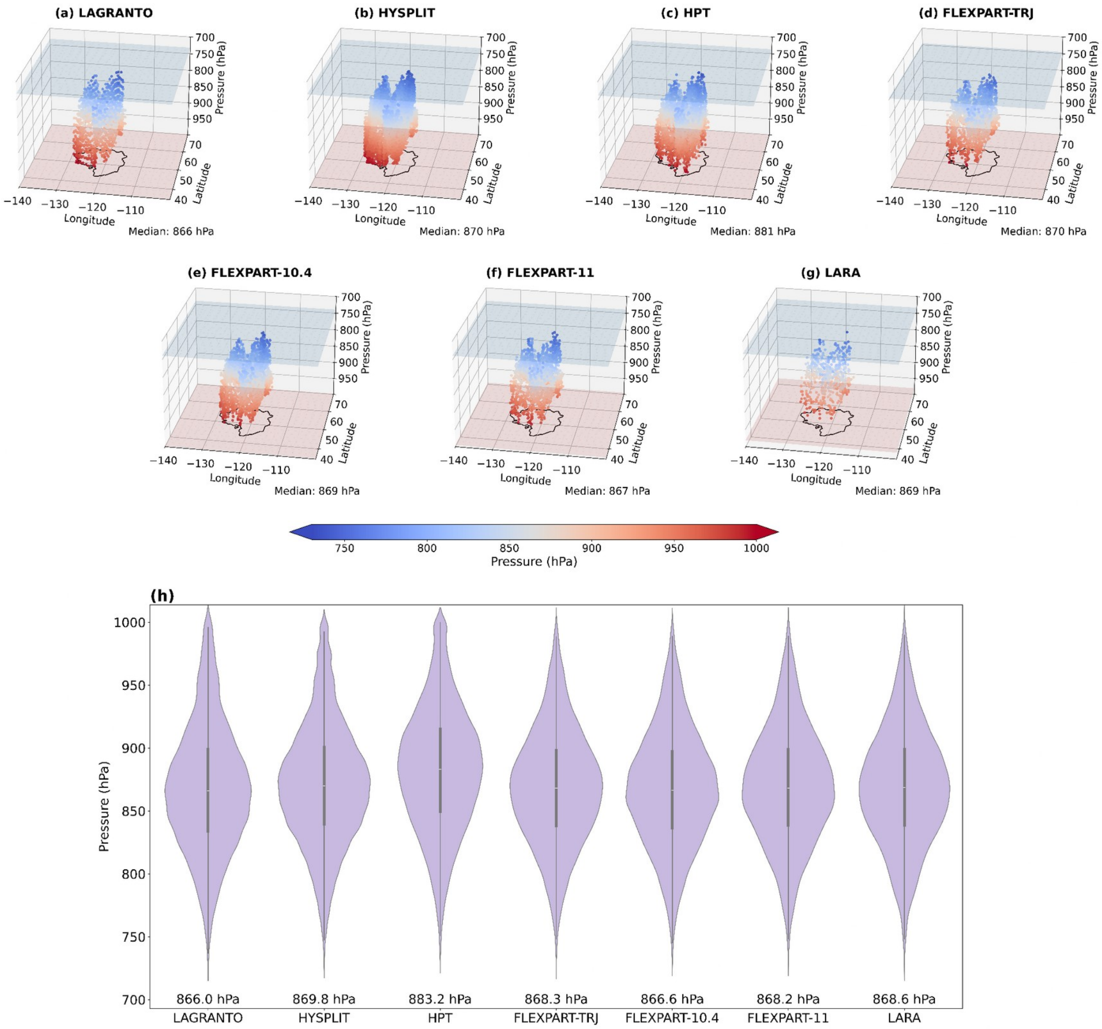

Figure 3: Three-dimensional distribution of Lagrangian air parcels within the 12 K temperature anomaly contour (black outline) at 00 UTC on 29 June 2021. Results are shown for (a) LAGRANTO, (b) HYSPLIT, (c) HPT, (d) FLEXPART-TRJ, (e) FLEXPART-10.4, (f) FLEXPART-11 and (g) LARA. Parcel positions are coloured by pressure (hPa). The median pressure across all parcels in each configuration is indicated below the respective panel. (h) Distribution of the vertical pressure (hPa) of all air parcels within the 12 K temperature anomaly contour from 28 to 30 June 2021 at 00, 06, 12, and 18 UTC. The mean value is shown as annotated text below each violin.

To further elucidate how these along-trajectory differences manifest in distinct air-mass histories, a cluster analysis of the parcel pathways is presented in Figure 4. All trajectories arriving within the 12 K temperature anomaly contour between 28 June 00 UTC and 30 June 18 UTC were included and grouped using a k-means clustering algorithm applied to the standardised

https://doi.org/10.5194/egusphere-2026-5144
Preprint. Discussion started: 8 September 2026

longitude–latitude time series of each parcel. Two dominant clusters emerged across all seven configurations: a primary cluster (C1) comprising 61–80% of parcels, and a secondary cluster (C2) accounting for the remainder. Despite subtle differences in the exact origin and curvature between models, the horizontal pathways (left column) indicate that both clusters originate broadly in the central-western North Pacific and approach the PNW21 HW region from the west or northwest.

The vertical evolution and accumulated process contributions (middle and right columns) reveal more pronounced differences between model classes (Figure 4). In the pure trajectory models, Cluster 1 parcels remain at relatively lower pressure levels (predominantly 800–900 hPa) throughout the 15-day backward period, with a gentle vertical slope in the days preceding arrival. This limited subsidence is consistent with the comparatively modest adiabatic contributions (10–26%) diagnosed in these models (Figure 2). By contrast, the dispersion models show that parcels in Cluster 1 originate at relatively mid-pressure levels (around 600 hPa) and undergo a steeper descent toward the surface, accompanied by substantial adiabatic warming (red shading) in the final days before arrival. This more pronounced subsidence aligns with the larger adiabatic fractions (44–49%) obtained from the dispersion-model decomposition (Figure 2). Cluster 2, in turn, is characterised by a broadly similar descent of air parcels toward the surface in the days before arrival and consistently strong advective contributions to the temperature anomaly. However, the adiabatic and diabatic partitioning differs markedly between model classes, with the pure trajectory models showing more pronounced diabatic warming and the dispersion models exhibiting stronger adiabatic contributions and even diabatic cooling.

The systematic difference in vertical histories between model classes is further illustrated in Figure 5, which shows the median horizontal position and pressure level of parcels 3 and 6 days before arrival at the 12 K temperature anomaly contour in the target region. Across all three days of the HW peak (28–30 June), the dispersion models consistently show parcels at higher altitudes than the pure trajectory models, while their horizontal positions remain clustered in similar regions. It is important to note that 6 days before arrival on June 28, the mean positions of HPT and FLEXPART-11 parcels differ somewhat from those of the other models (Figure 5a). Despite these differences, the budget contributions derived from HPT remain consistent with other pure trajectory models; similarly, the FLEXPART-11 results align with other dispersion simulations. This suggests that the parcel origin at longer lead times is not the dominant cause of the discrepancies in the relative contributions of the physical processes (Figure 1).

https://doi.org/10.5194/egusphere-2026-5144
Preprint. Discussion started: 8 September 2026

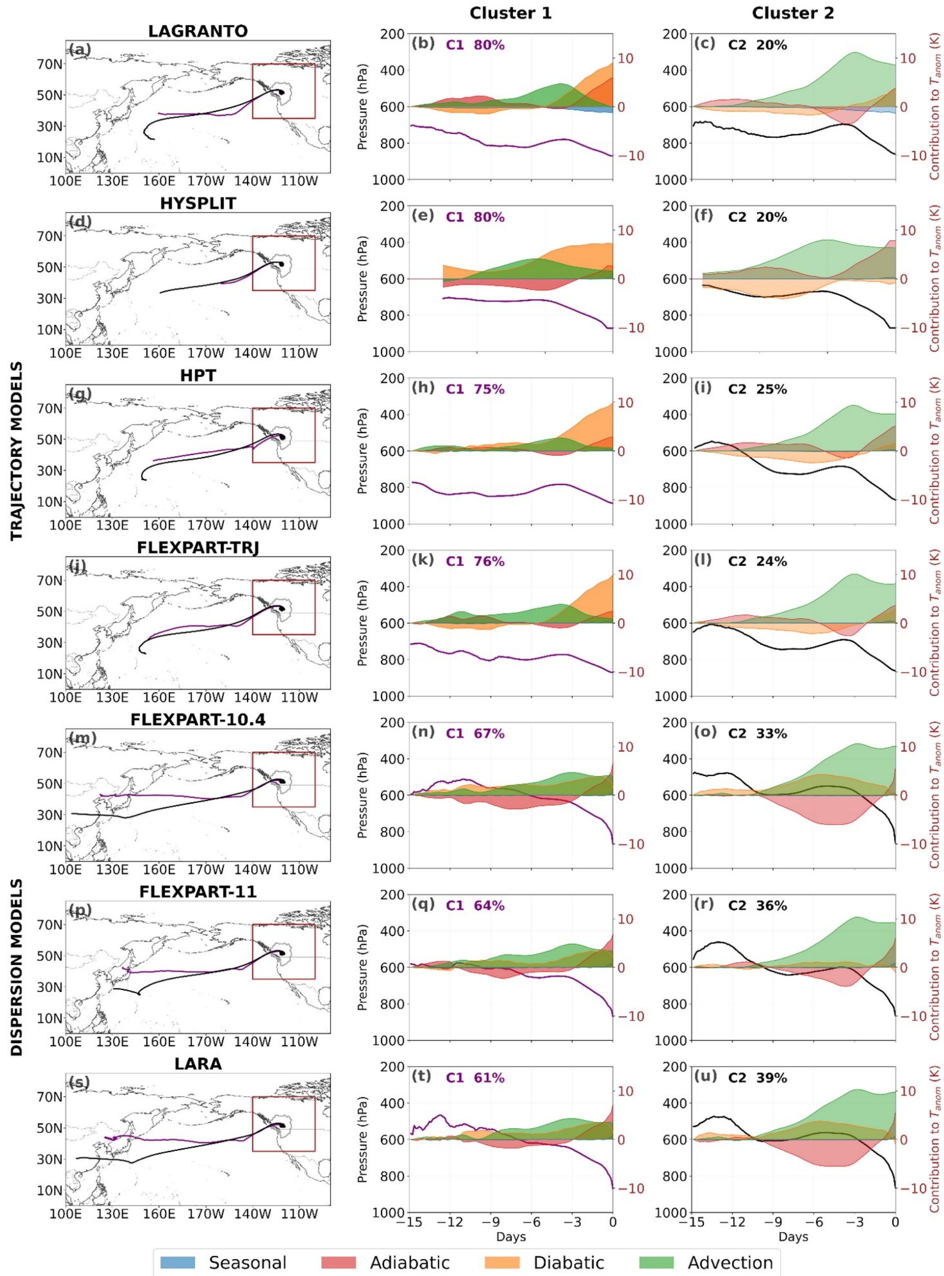

Figure 4: Cluster analysis of Lagrangian backward trajectories for air parcels arriving within the 12 K temperature anomaly contour (gray box in the left column) during the 28–30 June 2021 Pacific Northwest heatwave. (a, d, g, j, m, p, s) Mean horizontal pathways of the two dominant trajectory clusters for each model, with the black dot marking the arrival location within the target region. (b, e, h, k, n, q, t) Mean vertical evolution and process contributions for Cluster 1. (c, f, i, l, o, r, u) Same as the middle column but for Cluster 2. Coloured filled areas indicate the contribution of seasonal (blue), adiabatic (red), diabatic (orange) and advective (green) processes to the temperature anomaly.

https://doi.org/10.5194/egusphere-2026-5144
Preprint. Discussion started: 8 September 2026

Notably, for 29 and 30 June, the 3-day median positions lie almost directly over the PNW21 heatwave region, indicating that a substantial fraction of parcels resided within or near the target area for several days before the HW peak. It is noteworthy that the 3-day mean positions before arrival on 30 June from pure-trajectory models are broadly consistent with the median parcel altitudes at the target region during the HW dates (Figure 3), confirming that most parcels are near-surface. This pattern supports the larger diabatic contributions diagnosed by the pure trajectory models, as parcels remain within the heated boundary layer and are exposed to strong sensible heat fluxes from the warm land surface. In addition, the HW was preceded by anomalously dry conditions marked by precipitation deficits during spring, which reduced soil moisture across much of the region (Baier et al., 2023; Conrick and Mass, 2023), and favoured the rising near-surface temperatures through reduced evaporative cooling and increased sensible heat fluxes (Stéfanon et al., 2014; Miralles et al., 2014). In contrast, dispersion models simulate parcels slightly higher, reducing their residence time within the surface layer, thereby diminishing the accumulated diabatic signal and shifting the attribution toward adiabatic warming by subsidence.

https://doi.org/10.5194/egusphere-2026-5144
Preprint. Discussion started: 8 September 2026

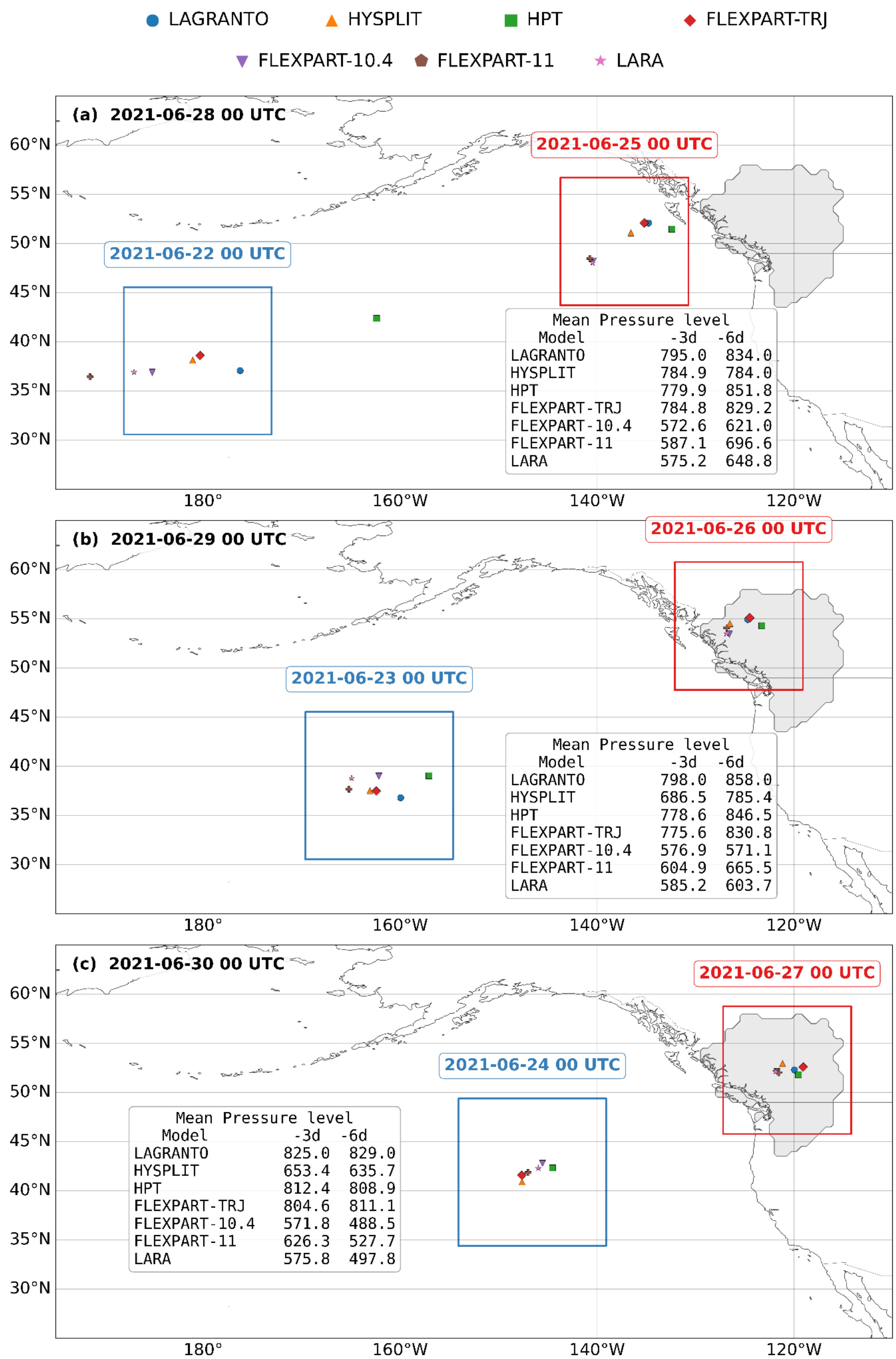

Figure 5: Median horizontal position and mean pressure level of Lagrangian air parcels 3 days (red boxes) and 6 days (blue boxes) before arrival within the 12 K temperature anomaly contour during the 28–30 June 2021 Pacific Northwest heatwave. Panels show arrivals on (a) 28

https://doi.org/10.5194/egusphere-2026-5144
Preprint. Discussion started: 8 September 2026

June 00 UTC, (b) 29 June 00 UTC and (c) 30 June 00 UTC. Symbols denote the median position for each model at the specified lead time; inset tables provide the mean pressure level (hPa) at 3 and 6 days before arrival.

Overall, this analysis demonstrates that the divergence in process attribution does not stem from different horizontal origins, but rather from contrasting vertical histories, specifically, the degree of subsidence experienced by the dominant air-mass trajectories. This finding is consistent with differences in how Lagrangian particle dispersion models and pure trajectory models represent sub-grid processes. While FLEXPART's stochastic turbulence and convection schemes introduce additional vertical dispersion, pure trajectory models rely solely on resolved grid-scale winds. Therefore, given that the parcel distributions over the target region are nevertheless similar across all configurations (Figure 3), the discrepancies in diagnosed adiabatic, diabatic and advective contributions arise not from where the parcels end up, but from how their thermodynamic histories are reconstructed along the trajectory from the genesis time. Thus, contrasting process attributions reflect the sensitivity of the Lagrangian temperature anomaly decomposition to the representation or neglect of subgrid motions, which could modulate the accumulation of heating and subsidence during air-mass transport.

3.3 Impact of FLEXPART parameterizations

Based on the previous analysis, the differences observed in the Lagrangian temperature anomaly decomposition are likely linked to turbulence and convection schemes in the FLEXPART model. To better understand which parameterisations lead to the discrepancies observed between the pure-trajectory models and dispersion models, we also performed an additional set of simulations following the description for FLEXPART-TRJ but switching on/off turbulence, mesoscale turbulence, convection, and subgrid orographic boundary layer height parameterisations, as shown in Table 1. When turbulence is switched on, air parcel motion is the sum of the grid-scale wind and turbulent wind fluctuations. In addition, mesoscale wind fluctuations are added to the parcel velocity through the mesoscale turbulence parameterisation. These mesoscale motions are neither resolved by the meteorological data nor covered by the turbulence scheme. Meanwhile, the convection scheme redistributes parcels vertically based on convective mass fluxes, and the subgrid orographic boundary layer height parameterisation increases the boundary layer height over which parcels are effectively mixed to account for subgrid-scale orographic variations.

Table 1: Selected configuration settings for the FLEXPART (v11) model simulation experiments, used to test the sensitivity of the Lagrangian temperature anomaly decomposition to increase in boundary layer height due to subgrid-scale orographic variations (SUBGRID), convection parameterization (CONVECTION), and mesoscale turbulence (TURBULENCE_MESO) and turbulence (TURBULENCE) parameterizations.

Simulation ID	SUBGRID	CONVECTION	TURBULENCE_MESO	TURBULENCE
no-TURB	ON	ON	ON	OFF
no-ALL_TURB	ON	ON	OFF	OFF

https://doi.org/10.5194/egusphere-2026-5144
Preprint. Discussion started: 8 September 2026

no-MESO	ON	ON	OFF	ON
no-CONV	ON	OFF	ON	ON
no-SUBGRID	OFF	ON	ON	ON

Figure 6 shows the six-hourly averaged Lagrangian temperature anomaly decomposition resulting from the additional FLEXPART model simulations outlined in Table 1. Simulations where turbulence is disabled (no-TURB and no-ALL_TURB) likely reproduce the diabatic-dominant behaviour observed in the pure-trajectory models (Figure 1). Collectively, these results isolate turbulence parameterisation as the primary driver of the discrepancies between the two model classes. This can be understood from the fact that, in FLEXPART, turbulence superimposes stochastic three-dimensional wind fluctuations onto the resolved flow via Langevin equations, causing air parcels to disperse vertically throughout the atmospheric column and sample thermodynamic environments different from those along the pure trajectory (Pisso et al., 2019; Bakels et al., 2024). In the boundary layer, turbulent mixing is represented by autocorrelated random perturbations with reflections at the surface and boundary layer top, while in the free troposphere fluctuations are driven by wind shear and stability, both of which drive parcels away from the grid-scale path (Pisso et al., 2019; Bakels et al., 2024). Consequently, the inclusion of stochastic turbulence allows parcels to disperse vertically and sample contrasting thermodynamic environments, effectively shifting the temperature anomaly budget from the diabatic-heating signature of pure trajectories toward the adiabatic-subsidence pattern observed in the full dispersion model. This demonstrates that the model-dependent divergence observed in Figure 1 originates fundamentally from the representation of turbulent transport, rather than from convection or mesoscale effects.

https://doi.org/10.5194/egusphere-2026-5144
Preprint. Discussion started: 8 September 2026

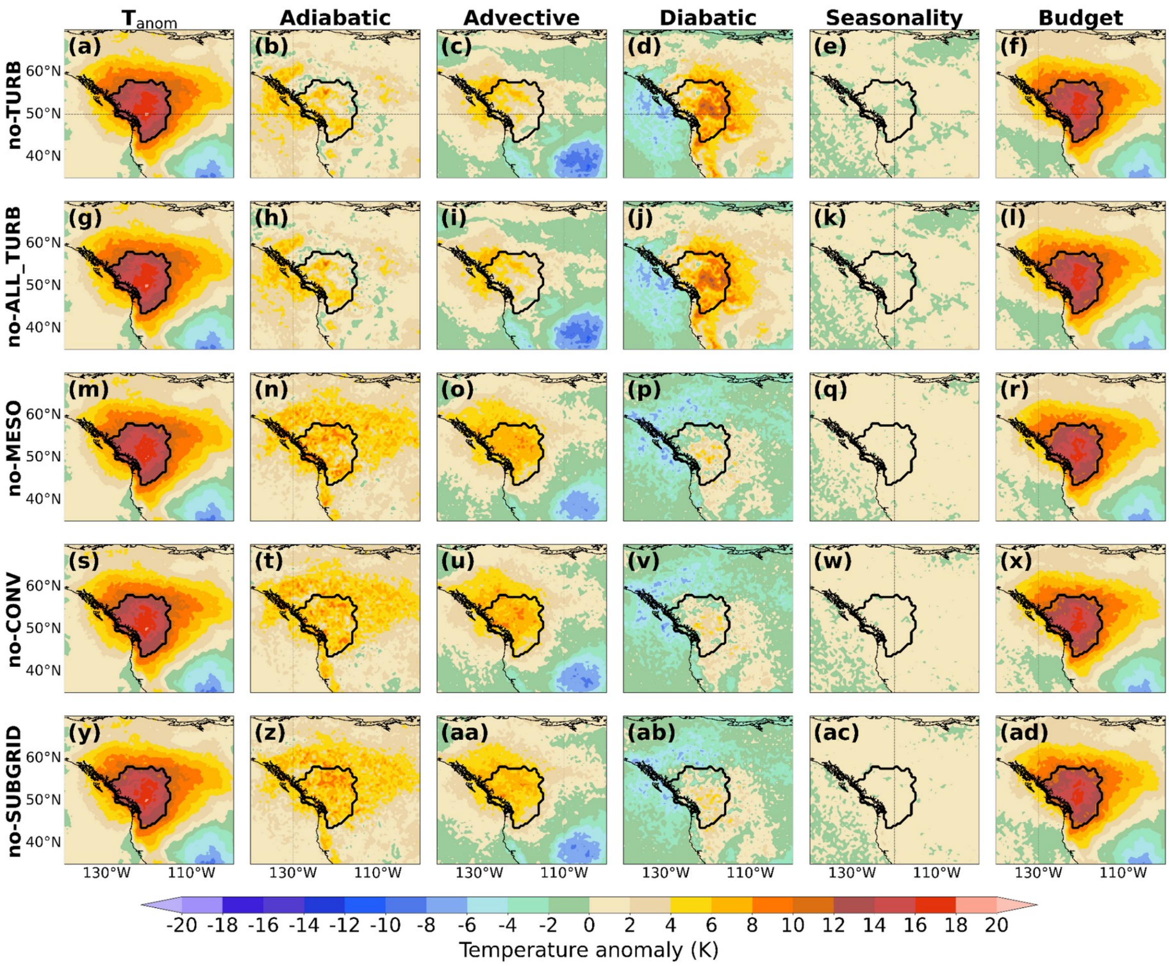

Figure 6: As Figure 1 but for the additional set of FLEXPART simulations switching off turbulence (no-TURB), all turbulence schemes (no-ALL_TURB), mesoscale turbulence (no-MESO), convection (no-CONV), and subgrid orographic boundary-layer height (no-SUBGRID).

In summary, a trajectory represents a mean air parcel moving through a well-mixed boundary layer, with boundaries open to subgrid-scale exchanges in pure-trajectory models (Sprenger and Wernli, 2015; Shukla et al., 2026). That is, in a well-mixed boundary layer heated by surface sensible heat fluxes, the air parcel will be heated through turbulent exchanges, showing up as diabatic T' as the air parcel moves with the mean flow through the boundary layer. Meanwhile, in dispersion models (with turbulence parameterisation set ON), trajectories follow the turbulent motions (not the mean flow) through the boundary layer and have closed boundaries with respect to turbulent exchanges (Stein et al., 2015; Pisso et al., 2019; Bakells et al., 2024). As a result, trajectories are generally diabatically heated only when located directly above the surface (or due to radiative or cloud processes). Consequently, these differences in the treatment of parcel motion alter the modelled vertical mixing and the spatial spread of trajectories, ultimately modulating their exposure to land-atmosphere feedbacks.

https://doi.org/10.5194/egusphere-2026-5144
Preprint. Discussion started: 8 September 2026

4 Final remarks and conclusions

The Lagrangian temperature anomaly decomposition has become an increasingly prominent tool for examining the physical drivers of heatwave events, offering process-level attribution of temperature extremes to adiabatic, advective, and diabatic contributions along air parcel trajectories (Röthlisberger and Papritz, 2023). However, this study reveals substantial discrepancies in process attribution using Lagrangian pure-trajectory or dispersion models (Figure 1). We used seven sets of air parcel trajectories: three from the FLEXPART dispersion model and four from pure trajectory models, including a FLEXPART simulation with all sub-grid parameterisations switched off. While the pure trajectory models consistently identify diabatic processes as the dominant contributor to the PNW21 heatwave, the dispersion models attribute the largest fraction of warming to adiabatic heating. Notably, the three-dimensional distribution of near-surface air parcels within the target region during the HW peak is broadly similar across all seven trajectory sets, with comparable median origins in the central-western North Pacific Ocean. This indicates that the divergence in process attribution does not stem from different geographic origins or vertical distributions over the target region, but rather from contrasting vertical histories during the backward trajectories. The median altitude of parcels in the dispersion models was substantially higher than in the pure trajectory models during the days before arrival (Figures 4 and 5), exposing them to greater subsidence warming. In contrast, near-surface parcels from pure trajectory models, particularly from 3 days before arrival on 29 and 30 June, were more strongly influenced by sensible heating and land–atmosphere feedbacks (Stéfanon et al., 2014; Miralles et al., 2014). This raises fundamental questions about the sensitivity of this Lagrangian-based process attribution to the representation of sub-grid turbulence, which alters the vertical position of air parcels.

The differences between dispersion and pure trajectory models extend beyond their numerical schemes to the physical processes they represent. FLEXPART, for example, incorporates stochastic turbulence parameterisations that account for unresolved sub-grid vertical motions and turbulent mixing (Pisso et al., 2019; Bakels et al., 2024), which enables tracing of air parcels from near the surface (Baier et al., 2023), whereas pure trajectory models are based on resolved grid-scale wind fields and cannot capture such mixing. Moreover, while convective transport schemes (Emanuel and Zivkovic-Rothman, 1999; Forster et al., 2007) resolve the smaller-scale vertical motion that pure trajectory models miss, they do not result in the discrepancies observed in the temperature anomaly budget. Consequently, differences in turbulence representation fundamentally reshape the vertical distribution of parcels throughout their backward evolution, thereby altering the accumulated heating and cooling histories that feed into the Lagrangian process attribution.

Overall, this study reveals a critical sensitivity in the relative contribution of adiabatic, advective and diabatic warming when applying a Lagrangian temperature anomaly decomposition (Röthlisberger and Papritz, 2023). The inferred process dominance depends fundamentally on whether a Lagrangian pure-trajectory or dispersion model is employed. However, given that this analysis is based on a single case study, these results should not be generalised. It is crucial to extend this assessment to a broader range of case studies, encompassing different geographic regions with varying land-surface characteristics (e.g., diverse vegetation cover) and climate regimes (e.g., semi-arid environments). This will help determine whether these

https://doi.org/10.5194/egusphere-2026-5144
Preprint. Discussion started: 8 September 2026

differences are unique to this exceptional HW event or represent a more systematic model dependency. Additionally, we acknowledge that while we only consider FLEXPART within the dispersion model class, it is widely used in Lagrangian trajectory analysis, and the availability of several datasets (e.g., Vázquez et al., 2024; Bakels et al., 2025; Deman et al., 2026) makes it an attractive choice for applying the Lagrangian temperature anomaly decomposition.

Finally, this study does not establish which model class is most suitable, it represents a first step toward systematically investigating these discrepancies. The growing body of HW attribution studies that rely on a single Lagrangian model should therefore be aware that the inferred dominance of adiabatic versus diabatic processes may reflect the choice of model class rather than the underlying physics alone. Future work should examine whether the vertical-history sensitivity identified here can be reconciled through modified decomposition formulations or hybrid Eulerian–Lagrangian frameworks that better capture the full tropospheric column. Ultimately, the question of which physical process drove a HW event may have no unique answer; it depends on the perspective (and the model) from which the event is examined.

Code and data availability

The European Centre for Medium-Range Weather Forecasts ERA5 reanalysis can be freely downloaded through the C3S Climate Data Store and https://doi.org/10.24381/cds.143582cf, respectively. The air parcels trajectories from LAGRANTO are available at https://doi.org/10.1038/s41561-023-01126-1, while the global outputs from the FLEXPART-10.3, FLEXPART-11 and LARA reanalysis are available at https://doi.org/10.5281/zenodo.13682647, https://doi.org/10.5194/essd-2026-115, and https://doi.org/10.5194/essd-17-4569-2025, respectively. The HPT source code is available at https://github.com/ManishShukla001/Hybrid-Parcel-Tracker---Main. The HYSPLIT, HPT and FLEXPART-TRJ trajectories are available upon request to the corresponding author. The Lagrangian atmospheric moisture and heat tracking (LATTIN) tool is accessible through its GitHub repository at https://github.com/apalarcon/LATTIN.

Author contributions

APA Writing – review & editing, Writing – original draft, Visualisation, Software, Methodology, Investigation, Data curation, Conceptualisation. **RN**: Writing – review & editing, Supervision, Methodology, Investigation. **LG**: Writing – review & editing, Supervision, Methodology, Investigation.

Competing interests

The authors declare that they have no known competing financial interests or personal relationships that could have appeared to influence the work reported in this paper.

https://doi.org/10.5194/egusphere-2026-5144
Preprint. Discussion started: 8 September 2026

Acknowledgements

This work is supported by the APALPADOR project (grant no. PID2024-155515NB-I00) funded by the Ministerio de Ciencia, Innovación y Universidades, Spain (MICIU/AEI/10.13039/501100011033) and the CERES project funded by the Xunta the Galicia (grant No. ED431F-2026/14). A.P-A. thanks the support from the Xunta de Galicia (Consellería de Cultura, Educación, Formación Profesional e Universidades) under the Postdoctoral Grant No. and ED481B−2023-016. EPhysLab members are also supported by the Xunta de Galicia under the Project ED431C2025/37 (Programa de Consolidación e Estructuración de Unidades de Investigación Competitivas (Grupos de Referencia Competitiva) and Consellería de Cultura, Educación e Universidade). We also thank Belinda Hotz (Institute for Atmospheric and Climate Science, ETH Zürich) for her valuable comments that helped improve this paper. This work has also been possible thanks to the computing resources and technical support provided by CESGA (Centro de Supercomputación de Galicia) and RES (Red Española de Supercomputación).

Financial support

This work is supported by the APALPADOR project (grant no. PID2024-155515NB-I00) funded by the Ministerio de Ciencia, Innovación y Universidades, Spain (MICIU/AEI/10.13039/501100011033) and by “ERDF/EU”, and the CERES project funded by the Xunta the Galicia (grant No. ED431F-2026/14).

References

Alcamo, J., Moreno, J. M., Nováky, B., Bindi, M., Corobov, R., Devoy, R. J., and Shvidenko, A.: Climate change 2007: impacts, adaptation and vulnerability. Contribution of working group II to the fourth assessment report of the intergovernmental panel on climate change, Cambridge University Press, 541–580, 2007.

Aldama-Campino, A., Döös, K., Kjellsson, J., and Jönsson, B.: TRACMASS: Formal release of version 7.0, https://doi.org/10.5281/zenodo.4337926, 2020.

Baier, K., Rubel, M., and Stohl, A.: The 3-week-long transport history and deep tropical origin of the 2021 extreme heat wave in the Pacific Northwest, Geophys. Res. Lett., 50, e2023GL105865, https://doi.org/10.1029/2023GL105865, 2023.

Bakels, L., Tatsii, D., Tipka, A., Thompson, R., Dütsch, M., Blaschek, M., Seibert, P., Baier, K., Bucci, S., Cassiani, M., Eckhardt, S., Groot Zwaaftink, C., Henne, S., Kaufmann, P., Lechner, V., Maurer, C., Mulder, M. D., Pisso, I., Plach, A., Subramanian, R., Vojta, M., and Stohl, A.: FLEXPART version 11: Improved accuracy, efficiency, and flexibility, Geosci. Model Dev., 17, 7595–7627, https://doi.org/10.5194/gmd-17-7595-2024, 2024.

Bakels, L., Blaschek, M., Dütsch, M., Plach, A., Lechner, V., Brack, G., Haimberger, L., and Stohl, A.: LARA: A Lagrangian Reanalysis based on ERA5 spanning from 1940 to 2023, Earth Syst. Sci. Data, 17, 4569–4594, https://doi.org/10.5194/essd-17-4569-2025, 2025.

https://doi.org/10.5194/egusphere-2026-5144
Preprint. Discussion started: 8 September 2026

Barriopedro, D., García-Herrera, R., Ordóñez, C., Miralles, D. G., and Salcedo-Sanz, S.: Heat Waves: Physical Understanding and Scientific Challenges, Rev. Geophys., 61, e2022RG000780, https://doi.org/10.1029/2022RG000780, 2023.

Barriopedro, D., Fischer, E. M., Luterbacher, J., Trigo, R. M., and García-Herrera, R.: The hot summer of 2010: redrawing the temperature record map of Europe, Science, 332, 220–224, https://doi.org/10.1126/science.1201224, 2011.

Berg, A., Lintner, B. R., Findell, K. L., Malyshev, S., Loikith, P. C., and Gentine, P.: Impact of soil moisture–atmosphere interactions on surface temperature distribution, J. Climate, 27, 7976–7993, https://doi.org/10.1175/JCLI-D-13-00591.1, 2014.

Bieli, M., Pfahl, S., and Wernli, H.: A Lagrangian investigation of hot and cold temperature extremes in Europe, Q. J. Roy. Meteor. Soc., 141, 98–108, https://doi.org/10.1002/qj.2339, 2014.

Brás, T. A., Seixas, J., Carvalhais, N., and Jägermeyr, J.: Severity of drought and heatwave crop losses tripled over the last five decades in Europe, Environ. Res. Lett., 16, 065012, https://doi.org/10.1088/1748-9326/abf004, 2021.

Breshears, D. D., Fontaine, J. B., Ruthrof, K. X., Field, J. P., Feng, X., Burger, J. R., Law, D. J., Kala, J., and Hardy, E. S.: Underappreciated plant vulnerabilities to heat waves, New Phytol., 231, 32–39, https://doi.org/10.1111/nph.17348, 2021.

Cassiani, M., Stohl, A., and Brioude, J.: Lagrangian stochastic modelling of dispersion in the convective boundary layer with skewed turbulence conditions and a vertical density gradient: Formulation and implementation in the FLEXPART model, Bound.-Lay. Meteorol., 154, 367–390, https://doi.org/10.1007/s10546-014-9976-5, 2015.

Conrick, R. and Mass, C. F.: The influence of soil moisture on the historic 2021 Pacific Northwest heatwave, Mon. Weather Rev., 151, 1213–1228, https://doi.org/10.1175/MWR-D-22-0253.1, 2023.

Deman, V. M., Insua-Costa, D., Keune, J., Koppa, A., and Miralles, D. G.: A four-decade global Lagrangian air-parcel trajectory dataset for atmospheric moisture and heat analysis, Earth Syst. Sci. Data, 18, 4593–4615, https://doi.org/10.5194/essd-18-4593-2026, 2026.

De Lima, C. Z., Buzan, J. R., Moore, F. C., Baldos, U. L. C., Huber, M., and Hertel, T. W.: Heat stress on agricultural workers exacerbates crop impacts of climate change, Environ. Res. Lett., 16, 044020, https://doi.org/10.1088/1748-9326/abeb9f, 2021.

Di Luca, A., de Elía, R., Bador, M., and Argüeso, D.: Contribution of mean climate to hot temperature extremes for present and future climates, Weather Clim. Extremes, 28, 100255, https://doi.org/10.1016/j.wace.2020.100255, 2020.

Dosio, A., Mentaschi, L., Fischer, E. M., and Wyser, K.: Extreme heat waves under 1.5 C and 2 C global warming, Environ. Res. Lett., 13, 054006, https://doi.org/10.1088/1748-9326/aab827, 2018.

Döös, K.: Interocean exchange of water masses, J. Geophys. Res., 100, 13499–13514, https://doi.org/10.1029/95JC00337, 1995.

Ebi, K. L., Capon, A., Berry, P., Broderick, C., de Dear, R., Havenith, G., and Jay, O.: Hot weather and heat extremes: health risks, Lancet, 398, 698–708, https://doi.org/10.1016/S0140-6736(21)01208-3, 2021.

Emanuel, K. A. and Živković-Rothman, M.: Development and evaluation of a convection scheme for use in climate models, J. Atmos. Sci., 56, 1766–1782, https://doi.org/10.1175/1520-0469(1999)056<1766:DAEOAC>2.0.CO;2, 1999.

https://doi.org/10.5194/egusphere-2026-5144
Preprint. Discussion started: 8 September 2026

Fernández-Alvarez, J. C., Nieto, R., Vicente-Serrano, S. M., Carvalho, D., and Gimeno, L.: Moisture and temperature sources were key drivers of the anomalies for the record-breaking of 2023 Amazon drought, Commun. Earth Environ., 6, 801, https://doi.org/10.1038/s43247-025-02771-7, 2025.

Fernández-Alvarez, J. C., Nieto, R., Vicente-Serrano, S. M., Carvalho, D., and Gimeno, L.: Brief communication: Atmospheric moisture and near-surface temperature anomalies: key drivers in the 2022 European mega-drought, Nat. Hazards Earth Syst. Sci., 26, 3741–3748, https://doi.org/10.5194/nhess-26-3741-2026, 2026.

Fischer, E. M., Seneviratne, S. I., Lüthi, D., and Schär, C.: Contribution of land-atmosphere coupling to recent European summer heat waves, Geophys. Res. Lett., 34, L06707, https://doi.org/10.1029/2006GL029068, 2007.

Fleishman, E., Rupp, D. E., Loikith, P. C., Bumbaco, K. A., and O'Neill, L. W.: Synthesis of publications on the anomalous June 2021 heat wave in the Pacific Northwest of the united States and Canada, Bull. Amer. Meteor. Soc., 106, E1155–E1174, https://doi.org/10.1175/BAMS-D-24-0188.1, 2025.

Font, R. A., Khamis, K., Milner, A. M., Smith, G. H. S., and Ledger, M. E.: Low flow and heatwaves alter ecosystem functioning in a stream mesocosm experiment, Sci. Total Environ., 777, 146067, https://doi.org/10.1016/j.scitotenv.2021.146067, 2021.

Forster, C., Stohl, A., and Seibert, P.: Parameterization of convective transport in a Lagrangian particle dispersion model and its evaluation, J. Appl. Meteorol. Climatol., 46, 403–422, https://doi.org/10.1175/JAM2470.1, 2007.

García-Herrera, R., Díaz, J., Trigo, R. M., Luterbacher, J., and Fischer, E. M.: A review of the European summer heat wave of 2003, Crit. Rev. Environ. Sci. Technol., 40, 267–306, https://doi.org/10.1080/10643380802238137, 2010.

Gimeno, L., Nieto, R., Eiras-Barca, J., Sorí, R., Stojanovic, M., Pérez-Alarcón, A., Fernández-Alvarez, J. C., Gimeno-Sotelo, L., Coll-Hidalgo, P., Álvarez-Socorro, G., and Vicente-Serrano, S. M.: Tracing atmospheric heat and moisture pathways to understand compound drought–heatwave events, Weather Clim. Extremes, 53, 100923, https://doi.org/10.1016/j.wace.2026.100923, 2026.

Hanna, S. R.: Applications in air pollution modeling, in: Atmospheric Turbulence and Air Pollution Modelling, edited by: Nieuwstadt, F. T. M. and van Dop, H., Springer Netherlands, 275–310, https://doi.org/10.1007/978-94-010-9112-1_7, 1984.

He, Y., Zhu, X., Sheng, Z., and He, M.: Resonant waves play an important role in the increasing heat waves in Northern Hemisphere mid-latitudes under global warming, Geophys. Res. Lett., 50, e2023GL104839, https://doi.org/10.1029/2023GL104839, 2023.

Hersbach, H., Bell, B., Berrisford, P., Hirahara, S., Horányi, A., Muñoz-Sabater, J., Nicolas, J., Peubey, C., Radu, R., Schepers, D., Simmons, A., Soci, C., Abdalla, S., Abellan, X., Balsamo, G., Bechtold, P., Biavati, G., Bidlot, J., Bonavita, M., and Thépaut, J. N.: The ERA5 global reanalysis, Q. J. Roy. Meteor. Soc., 146, 1999–2049, https://doi.org/10.1002/qj.3803, 2020.

Hotz, N., Röthlisberger, M., and Papritz, L.: Understanding the vertical temperature structure of recent heat waves, Weather Clim. Dynam., 5, 323–344, https://doi.org/10.5194/wcd-5-323-2024, 2024.

https://doi.org/10.5194/egusphere-2026-5144
Preprint. Discussion started: 8 September 2026

Jia, X., Dong, W., Wu, R., Liu, F., and Wang, M.: Anthropogenic Warming Amplifies the Impact of the Tibetan Plateau Snow Cover on Eastern Europe Heat Waves, J. Climate, 39, 551–569, https://doi.org/10.1175/JCLI-D-25-0447.1, 2026.

Legras, B., Joseph, B., and Lefèvre, F.: Vertical diffusivity in the lower stratosphere from Lagrangian back-trajectory reconstructions of ozone profiles, J. Geophys. Res., 108, 4567, https://doi.org/10.1029/2002JD003045, 2003.

Lemburg, A., Fink, A. H., Lima, M. M., and Pinto, J. G.: Lagrangian analysis of two flavours of Central European heatwaves: Formation under omega blocking versus initiation by subtropical ridges, Q. J. Roy. Meteor. Soc., e70199, https://doi.org/10.1002/qj.70199, 2026.

Li, H., Keune, J., Gou, Q., Holgate, C. M., and Miralles, D.: Heat and moisture anomalies during crop failure events in the Southeastern Australian wheat belt, Earth's Future, 12, e2023EF003901, https://doi.org/10.1029/2023EF003901, 2024.

Lin, H., Mo, R., and Vitart, F.: The 2021 western North American heatwave and its subseasonal predictions, Geophys. Res. Lett., 49, e2021GL097036, https://doi.org/10.1029/2021GL097036, 2022.

Mass, C., Ovens, D., Christy, J., and Conrick, R.: The Pacific Northwest heat wave of 25–30 June 2021: Synoptic/mesoscale conditions and climate perspective, Weather Forecast., 39, 275–291, https://doi.org/10.1175/WAF-D-23-0154.1, 2024.

Mayer, A. and Wirth, V.: Two different perspectives on heatwaves within the Lagrangian framework, Weather Clim. Dynam., 6, 131–150, https://doi.org/10.5194/wcd-6-131-2025, 2025.

Maryon, R. H.: Determining cross-wind variance for low frequency wind meander, Atmos. Environ., 32, 115–121, https://doi.org/10.1016/S1352-2310(97)00325-7, 1998.

Miralles, D. G., Gentine, P., Seneviratne, S. I., and Teuling, A. J.: Land–atmospheric feedbacks during droughts and heatwaves: State of the science and current challenges, Ann. NY Acad. Sci., 1436, 19–35, https://doi.org/10.1111/nyas.13912, 2019.

Miralles, D. G., Teuling, A. J., Van Heerwaarden, C. C., and Vilà-Guerau de Arellano, J.: Mega-heatwave temperatures due to combined soil desiccation and atmospheric heat accumulation, Nat. Geosci., 7, 345–349, https://doi.org/10.1038/ngeo2141, 2014.

Moritz, M. A., Morais, M. E., Summerell, L. A., Carlson, J. M., and Doyle, J.: Wildfires, complexity, and highly optimized tolerance, P. Natl. Acad. Sci. USA, 102, 17912–17917, https://doi.org/10.1073/pnas.0508985102, 2005.

Mario, E., Raffaele, L., Onofrio, C., Maria, C. J., Valentina, B., Vincenzo, G., Shao, C., and Giovanni, S.: Coupling heat wave and wildfire occurrence across multiple ecoregions within a Eurasia longitudinal gradient, Sci. Total Environ., 912, 169269, https://doi.org/10.1016/j.scitotenv.2023.169269, 2024.

McKinnon, K. A. and Simpson, I. R.: How unexpected was the 2021 Pacific Northwest heatwave?, Geophys. Res. Lett., 49, e2022GL100380, https://doi.org/10.1029/2022GL100380, 2022.

Neal, E., Huang, Y. C. S., and Nakamura, N.: The 2021 Pacific Northwest Heat Wave and Associated Blocking: Meteorology and the Role of an Upstream Cyclone as a Diabatic Source of Wave Activity, Geophys. Res. Lett., 49, e2021GL097699, https://doi.org/10.1029/2021GL097699, 2022.

https://doi.org/10.5194/egusphere-2026-5144
Preprint. Discussion started: 8 September 2026

Oppong, F. B., Gonzalez, S., Hibbert, K., Méndez-Lázaro, P. A., and González-Cruz, J. E.: Climatology and Large-Scale Drivers of Extreme Heatwaves in the Caribbean: From 1971 to 2025, Geophys. Res. Lett., 52, e2025GL117649, https://doi.org/10.1029/2025GL117649, 2025.

Oertel, A., Pickl, M., Quinting, J. F., Hauser, S., Wandel, J., Magnusson, L., Balmaseda, M., Vitart, F., and Grams, C. M.: Everything Hits at Once: How Remote Rainfall Matters for the Prediction of the 2021 North American Heat Wave, Geophys. Res. Lett., 50, e2022GL100958, https://doi.org/10.1029/2022GL100958, 2023.

Papritz, L. and Röthlisberger, M.: A Novel Temperature Anomaly Source Diagnostic: Method and Application to the 2021 Heatwave in the Pacific Northwest, Geophys. Res. Lett., 50, e2023GL105641, https://doi.org/10.1029/2023GL105641, 2023.

Pascaline, W. and Rowena, H.: Economic losses, poverty and disaster 1998–2017, UNISDR, Geneva, 33, 2018.

Pérez-Alarcón, A., Vázquez, M., Ramos, A. M., Nieto, R., Pinto, J. G., and Gimeno, L.: Quantifying moisture and sensible heat flux anomalies for compound drought and heat wave events in the Iberian Peninsula, Weather Clim. Extremes, 47, 100756, https://doi.org/10.1016/j.wace.2025.100756, 2025.

Pérez-Alarcón, A., Sorí, R., Stojanovic, M., Lobaina-Castillo, D., Velázquez-Zaldivar, B., Trigo, R. M., Nieto, R., and Gimeno, L.: The relative contribution of physical processes leading the May 2024 heat wave in Cuba using a novel temperature anomaly analysis, Weather Clim. Extremes, 50, 100827, https://doi.org/10.1016/j.wace.2025.100827, 2025.

Pérez-Alarcón, A., Nieto, R., and Gimeno, L.: Version (1.1.10) — LATTIN: A Python-based tool for Lagrangian atmospheric moisture and heat tracking, Softw. Impacts, 28, 100834, https://doi.org/10.1016/j.simpa.2026.100834, 2026.

Pérez-Alarcón, A., Fernández-Alvarez, J. C., Nieto, R., and Gimeno, L.: LATTIN: A Python-based tool for Lagrangian atmospheric moisture and heat tracking, Softw. Impacts, 20, 100638, https://doi.org/10.1016/j.simpa.2024.100638, 2024.

Perkins, S. E.: A review on the scientific understanding of heatwaves—Their measurement, driving mechanisms, and changes at the global scale, Atmos. Res., 164-165, 242–267, https://doi.org/10.1016/j.atmosres.2015.05.014, 2015.

Pfahl, S. and Wernli, H.: Quantifying the relevance of atmospheric blocking for co-located temperature extremes in the Northern Hemisphere on (sub-)daily time scales, Geophys. Res. Lett., 39, L12807, https://doi.org/10.1029/2012GL052261, 2012.

Philip, S. Y., Kew, S. F., van Oldenborgh, G. J., Anslow, F. S., Seneviratne, S. I., Vautard, R., Coumou, D., Ebi, K. L., Arrighi, J., Singh, R., van Aalst, M., Pereira Marghidan, C., Wehner, M., Yang, W., Li, S., Schumacher, D. L., Hauser, M., Bonnet, R., Luu, L. N., and Otto, F. E. L.: Rapid attribution analysis of the extraordinary heatwave on the Pacific Coast of the US and Canada June 2021, Earth Syst. Dynam., 13, 1689–1713, https://doi.org/10.5194/esd-13-1689-2022, 2022.

Pisso, I., Sollum, E., Grythe, H., Kristiansen, N. I., Cassiani, M., Eckhardt, S., Arnold, D., Morton, D., Thompson, R. L., Groot Zwaaftink, C. D., Evangeliou, N., Sodemann, H., Haimberger, L., Henne, S., Brunner, D., Burkhart, J. F., Fouilloux, A., Brioude, J., Philipp, A., and Stohl, A.: The Lagrangian particle dispersion model FLEXPART version 10.4, Geosci. Model Dev., 12, 4955–4997, https://doi.org/10.5194/gmd-12-4955-2019, 2019.

https://doi.org/10.5194/egusphere-2026-5144
Preprint. Discussion started: 8 September 2026

Qian, Y., Hsu, P. C., Yuan, J., Zhu, Z., Wang, H., and Duan, M.: Effects of subseasonal variation in the East Asian monsoon system on the summertime heat wave in western North America in 2021, Geophys. Res. Lett., 49, e2021GL097659, https://doi.org/10.1029/2021GL097659, 2022.

Quinting, J. F. and Reeder, M. J.: Southeastern Australian heat waves from a trajectory viewpoint, Mon. Weather Rev., 145, 4109–4125, https://doi.org/10.1175/MWR-D-17-0165.1, 2017.

Robinson, P. J.: On the definition of a heat wave, J. Appl. Meteorol., 40, 762–775, https://doi.org/10.1175/1520-0450(2001)040<0762:OTDOAH>2.0.CO;2, 2001.

Ruffault, J., Curt, T., Moron, V., Trigo, R. M., Mouillot, F., Koutsias, N., Pimont, F., Martin-StPaul, N., Barbero, R., Dupuy, J. L., Russo, A., and Belhadj-Khedher, C.: Increased likelihood of heat-induced large wildfires in the Mediterranean Basin, Sci. Rep., 10, 13790, https://doi.org/10.1038/s41598-020-70069-z, 2020.

Ruffault, J., Moron, V., Trigo, R. M., and Curt, T.: Daily synoptic conditions associated with large fire occurrence in Mediterranean France: Evidence for a wind-driven fire regime, Int. J. Climatol., 37, 524–533, https://doi.org/10.1002/joc.4680, 2016.

Röthlisberger, M. and Papritz, L.: Quantifying the physical processes leading to atmospheric hot extremes at a global scale, Nat. Geosci., 16, 210–216, https://doi.org/10.1038/s41561-023-01126-1, 2023.

Ryall, D. B. and Maryon, R. H.: Validation of the UK Met. Office's NAME model against the ETEX dataset, Atmos. Environ., 32, 4265–4276, https://doi.org/10.1016/S1352-2310(98)00177-0, 1998.

Santos, J. A., Pfahl, S., Pinto, J. G., and Wernli, H.: Mechanisms underlying temperature extremes in Iberia: a Lagrangian perspective, Tellus A, 67, 26032, https://doi.org/10.3402/tellusa.v67.26032, 2015.

Schaller, N., Sillmann, J., Anstey, J., Fischer, E. M., Grams, C. M., and Russo, S.: Influence of blocking on Northern European and Western Russian heatwaves in large climate model ensembles, Environ. Res. Lett., 13, 054015, https://doi.org/10.1088/1748-9326/aaba55, 2018.

Schumacher, D. L., Keune, J., Van Heerwaarden, C. C., Teuling, A. J., and Miralles, D. G.: Amplification of mega-heatwaves through heat torrents fuelled by upwind drought, Nat. Geosci., 12, 712–717, https://doi.org/10.1038/s41561-019-0431-6, 2019.

Schumacher, D. L., Keune, J., and Miralles, D. G.: Atmospheric heat and moisture transport to energy- and water-limited ecosystems, Ann. NY Acad. Sci., 1472, 123–138, https://doi.org/10.1111/nyas.14357, 2020.

Schumacher, D. L., Hauser, M., and Seneviratne, S. I.: Drivers and mechanisms of the 2021 Pacific Northwest heatwave, Earth's Future, 10, e2022EF002967, https://doi.org/10.1029/2022EF002967, 2022.

Shukla, M., Ganapathiraju, S. A., Pérez-Alarcón, A. , and Rathinasamy, M.: Hybrid Parcel Tracker (HPT) – A Python-based framework to analyse moisture movement during extreme precipitation events, Atmos. Res., 342, 109136, https://doi.org/10.1016/j.atmosres.2026.109136, 2026.

https://doi.org/10.5194/egusphere-2026-5144
Preprint. Discussion started: 8 September 2026

Sousa, P. M., Barriopedro, D., Ramos, A. M., García-Herrera, R., Espírito-Santo, F., and Trigo, R. M.: Saharan air intrusions as a relevant mechanism for Iberian heatwaves: The record breaking events of August 2018 and June 2019, Weather Clim. Extremes, 26, 100224, https://doi.org/10.1016/j.wace.2019.100224, 2019.

Sousa, P. M., Trigo, R. M., Barriopedro, D., Soares, P. M. M., and Santos, J. A.: European temperature responses to blocking and ridge regional patterns, Clim. Dynam., 50, 457–477, https://doi.org/10.1007/s00382-017-3620-2, 2018.

Sprenger, M. and Wernli, H.: The LAGRANTO Lagrangian analysis tool–version 2.0, Geosci. Model Dev., 8, 2569–2586, https://doi.org/10.5194/gmd-8-2569-2015, 2015.

Stéfanon, M., Drobinski, P., D'Andrea, F., Lebeaupin-Brossier, C., and Bastin, S.: Soil moisture-temperature feedbacks at meso-scale during summer heat waves over Western Europe, Clim. Dynam., 42, 1309–1324, https://doi.org/10.1007/s00382-013-1794-9, 2014.

Stein, A. F., Draxler, R. R., Rolph, G. D., Stunder, B. J. B., Cohen, M. D., and Ngan, F.: NOAA's HYSPLIT atmospheric transport and dispersion modeling system, Bull. Amer. Meteor. Soc., 96, 2059–2077, https://doi.org/10.1175/BAMS-D-14-00110.1, 2015.

Stohl, A., Hittenberger, M., and Wotawa, G.: Validation of the lagrangian particle dispersion model FLEXPART against large-scale tracer experiment data, Atmos. Environ., 32, 4245–4264, https://doi.org/10.1016/S1352-2310(98)00184-8, 1998.

Stohl, A., Forster, C., Frank, A., Seibert, P., and Wotawa, G.: The Lagrangian particle dispersion model FLEXPART version 6.2, Atmos. Chem. Phys., 5, 2461–2474, https://doi.org/10.5194/acp-5-2461-2005, 2005.

Stone Jr, B., Mallen, E., Rajput, M., Gronlund, C. J., Broadbent, A. M., Krayenhoff, E. S., and Georgescu, M.: Compound climate and infrastructure events: how electrical grid failure alters heat wave risk, Environ. Sci. Technol., 55, 6957–6964, https://doi.org/10.1021/acs.est.1c00024, 2021.

Sutanto, S. J., Vitolo, C., Di Napoli, C., D'Andrea, M., and van Lanen, H. A. J.: Heatwaves, droughts, and fires: Exploring compound and cascading dry hazards at the pan-European scale, Environ. Int., 134, 105276, https://doi.org/10.1016/j.envint.2019.105276, 2020.

Tamarin-Brodsky, T., Hodges, K., Hoskins, B. J., and Shepherd, T. G.: Changes in Northern Hemisphere temperature variability shaped by regional warming patterns, Nat. Geosci., 13, 414–421, https://doi.org/10.1038/s41561-020-0576-3, 2020.

Terray, L.: A storyline approach to the June 2021 northwestern North American heatwave, Geophys. Res. Lett., 50, e2022GL101640, https://doi.org/10.1029/2022GL101640, 2023.

Vázquez, M., Alvarez-Socorro, G., Fernández-Alvarez, J. C., Nieto, R., and Gimeno, L.: Global FLEXPART-ERA5 simulations using 30 million atmospheric parcels since 1980, Zenodo, https://doi.org/10.5281/zenodo.13682647, 2024.

Vogel, M. M., Zscheischler, J., Wartenburger, R., Dee, D., and Seneviratne, S. I.: Concurrent 2018 Hot Extremes Across Northern Hemisphere Due to Human-Induced Climate Change, Earth's Future, 7, 692–703, https://doi.org/10.1029/2019EF001189, 2019.

https://doi.org/10.5194/egusphere-2026-5144
Preprint. Discussion started: 8 September 2026

Wehrli, K., Luo, F., Hauser, M., Shiogama, H., Tokuda, D., Kim, H., and Seneviratne, S. I.: The ExtremeX global climate model experiment: investigating thermodynamic and dynamic processes contributing to weather and climate extremes, Earth Syst. Dynam., 13, 1167–1196, https://doi.org/10.5194/esd-13-1167-2022, 2021.

White, R. H., Anderson, S., Booth, J. F., Braich, G., Draeger, C., Fei, C., Harley, C. D., Henderson, S. B., Jakob, M., Lau, C. A., Mareshet Admasu, L., Narinesingh, V., Rodell, C., Roocroft, E., Weinberger, K. R., and West, G.: The unprecedented Pacific Northwest heatwave of June 2021, Nat. Commun., 14, 727, https://doi.org/10.1038/s41467-023-36289-3, 2023.

Zhou, S., Williams, A. P., Berg, A. M., Cook, B. I., Zhang, Y., Hagemann, S., Lorenz, R., Seneviratne, S. I., and Gentine, P.: Land–atmosphere feedbacks exacerbate concurrent soil drought and atmospheric aridity, P. Natl. Acad. Sci. USA, 116, 18848–18853, https://doi.org/10.1073/pnas.1904955116, 2019.

Zhou, S. and Yuan, X.: Upwind Droughts Enhance Half of the Heatwaves Over North China, Geophys. Res. Lett., 49, e2021GL096639, https://doi.org/10.1029/2021GL096639, 2022.

Zhou, S., Liang, M., and Yuan, X.: Impact of upwind flash drought on 2022 record-shattering heatwave over East China, Clim. Dynam., 62, 6367–6380, https://doi.org/10.1007/s00382-024-07211-4, 2024.

Zschenderlein, P., Pfahl, S., Wernli, H., and Fink, A. H.: A Lagrangian analysis of upper-tropospheric anticyclones associated with heat waves in Europe, Weather Clim. Dynam., 1, 191–206, https://doi.org/10.5194/wcd-1-191-2020, 2020.